JACS
JOURNAL OF THE AMERICAN CHEMICAL SOCIETY

Communication

pubs.acs.org/JACS

Stability and Kinetics of c-*MYC* Promoter G-Quadruplexes Studied by Single-Molecule Manipulation

Huijuan You,[†] Jingyuan Wu,[‡] Fangwei Shao,[‡] and Jie Yan*[,†,∥,§]

[†]Mechanobiology Institute, National University of Singapore, 117411, Singapore

[‡]Division of Chemistry and Biological Chemistry, School of Physical and Mathematical Sciences, Nanyang Technological University, 21 Nanyang Link, 637371, Singapore

[∥]Department of Physics, National University of Singapore, 117542, Singapore

[§]Centre for Bioimaging Sciences, National University of Singapore, 117546, Singapore

Supporting Information

ABSTRACT: A DNA G-quadruplex (G4) formed at the oncogene c-*MYC* promoter region functions as a gene silencer. Due to its high stability at physiological K^+ concentrations, its thermodynamics and kinetic properties have not been characterized in physiological solution conditions. In this work, we investigated the unfolding and folding transitions of single c-*MYC* G4 and several of its truncated or point mutants at 100 mM KCl concentration under mechanical force. We found that the wild type could fold into multiple species, and the major specie has a slow unfolding rate of $(1.4 \pm 1.0) \times 10^{-6}$ s^{-1}. The force-dependent thermodynamics and kinetic properties of the major specie were obtained by studying a truncated mutant, Myc2345, that contains the G-tracts 2, 3, 4, and 5. As the c-*MYC* G4 is a prototype of many other intermolecular parallel-stranded G4's, our results provide important insights into the stability of a broad class of promoter G4's which also play a role in transcription regulation and are potential anticancer targets.

Guanine-rich DNA sequences ($G_{\geq 3}N_xG_{\geq 3}N_xG_{\geq 3}N_xG_{\geq 3}$) containing four or more G tracts ($G_{\geq 3}$, more than three guanines) and loop regions (N_x, typically 1−7 nucleotides) have the potential to form four-stranded G-quadruplex (G4) structures, which are stabilized by Hoogsteen H-bonds and central cations such as K^+ or Na^+.[1] G4 structures have drawn increasing attention, as the potential G4-forming sequences are widespread in the human genome, including the human telomere region, and in the promoter regions of numerous genes including many oncogenes.[2]

The c-*MYC* G4 formed on the 27-bp purine-rich sequence, also known as nuclease hypersensitivity element III_1 (NHE III_1), is located at 142−115 bp upstream from the P1 promoter of c-*MYC* gene.[3] The c-*MYC* gene encodes a 65 kDa nuclear phosphoro-protein (transcription factor), which is a central regulator of cell growth, proliferation, differentiation, and apoptosis.[4] Overexpression of the c-*MYC* gene is related to various cancers.[5] The c-*MYC* G4 formed on NHE III_1 region acts as a transcription repressor and controls about 75−85% of c-*MYC* transcription.[3,6]

The c-*MYC* G4 is highly stable and can remain in folded conformations near the boiling temperature in physiological K^+ concentrations of ∼100 mM. Destabilizing the c-*MYC* G4 by replacing a single guanine with adenine (G17A) can resume the transcription.[7] In addition, small ligands stabilizing the c-*MYC* G4 have been shown to downregulate the expression of the c-*MYC* gene in lymphoma cell line, offering promise for cancer therapeutics.[7] Thus, characterizing the stability of c-*MYC* G4 is important for understanding its transcriptional regulation mechanism and for designing anticancer drugs.

The stability of G4 has been studied using UV, CD, and NMR spectroscopy during changing temperatures.[8] However, due to its high stability in physiological K^+ concentration, the melting transition of c-*MYC* G4 cannot reach completion even at boiling temperature,[9] thus causing uncertainty in melting temperature measurements. In addition, the folding/unfolding kinetics of c-*MYC* G4 in physiological relevant buffer condition has not been characterized yet.

In this report, using an in-house-made magnetic tweezers,[11] we investigated the stability of c-*MYC* G4 formed on the wild-type (wt) sequence Pu27, which contains five G-tracts, two truncated mutants Myc2345 and Myc1245, each containing a subset of four G-tracts, and a single guanine replacement mutant Pu27-G17A (Figure 1A). Single-strand Pu27 sequence has been shown able to fold into at least two types of G4 structures in 100 mM K^+ solution.[7] Dimethyl sulfate (DMS) footprinting analysis has suggested that the major form involves the G-tracts 2, 3, 4, and 5 and the minor form involves G-tracts 1, 2, 4, and 5.[7] The G4 structures formed on the mutants Myc2345 and Myc1245 (the numbers indicate the number of G-tracts involved) are both parallel structures with all strands oriented in the same direction and the glycosidic bonds all *anti*. The only structural difference between Myc1245 G4 and Myc2345 G4 is that the former has a longer middle loop than that of the latter[12] (Figure 1B). Despite their structural similarity, they have markedly different stability with 15 degrees higher T_m measured for Myc2345 G4 than for Myc1245 G4 in 9 mM KCl.[12a]

Our CD spectra of the structures formed on all the sequences show a minimum at 235 nm and a maximum at

Received: November 13, 2014
Published: February 5, 2015

DOI: 10.1021/ja511680u
J. Am. Chem. Soc. 2015, 137, 2424−2427

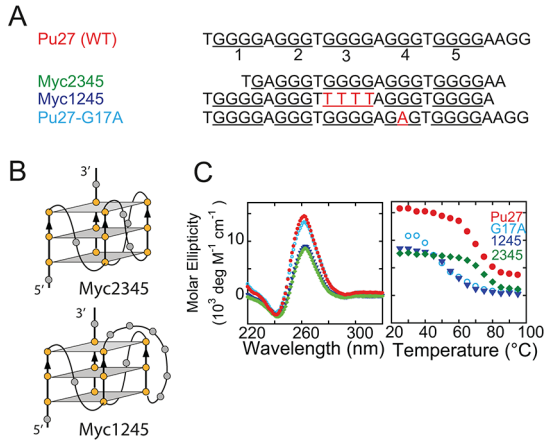

Figure 1. c-*MYC* G4 DNA sequences, structures and CD spectra. (A) The NHE III_1 G-rich strand of the c-*MYC* gene and its mutants: Pu27, the 27-nt wild-type sequence; Myc2345, a truncated mutant containing G-tracts 2, 3, 4, and 5; Myc1245, the G-tract 3 is substituted by four T; and Pu27-G17A, a substitution mutant with a single G-to-A mutation on the G-tract 4. (B) Schematic structures of Myc2345 and Myc1245 according to previous NMR studies.[12] (C) Left, CD spectra of Pu27 (red), Myc2345 (green), Myc1245 (blue), and Pu27-G17A (cyan) DNA in 100 mM KCl at 25 °C. Right, CD melting curves of Pu27 (red), Myc2345 (green), Myc1245 (blue), and Pu27-G17A (cyan) measured in 20 mM KCl.

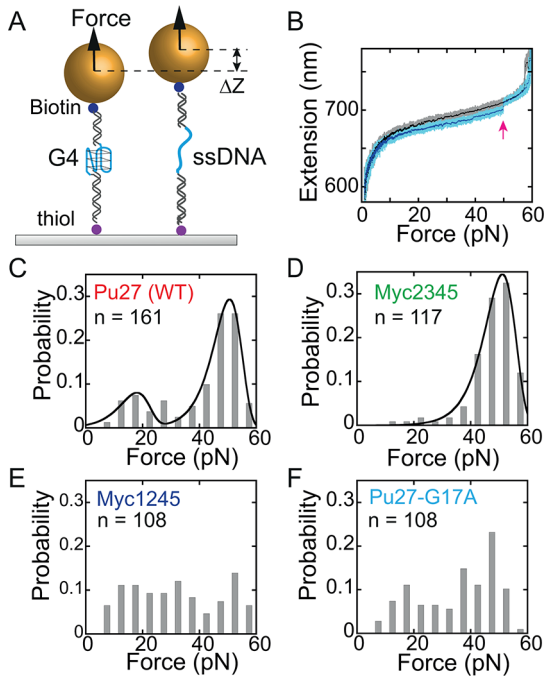

Figure 2. Unfolding force distributions (A) Schematic of the magnetic tweezers measurement. The G4 ssDNA sequences are flanked between two dsDNA handles (1449bp and 601 bp) and are tethered between a paramagnetic bead and coverslip. (B) Typical force extension curves (force-increase scan, cyan; force-decrease scan, gray).The black and blue showed the smoothed data. G4 unfolding results in a sudden extension jump (red arrow) in the force-increase curve. (C–F) Unfolding force histograms for the Pu27 (C), mutants Myc2345 (D), Myc1245 (E), and Pu27-G17A (F).

260 nm, which indicates formation of parallel-stranded G4 structures (Figure 1C).[8] The G4 structures remain folded even at 95 °C in the presence of 100 mM KCl (100 mM KCl, 10 mM Tris-HCl, pH 8.0). In lower KCl concentration of 20 mM, the CD melting curves show that Pu27 G4 and Myc2345 G4 have a similar T_m of 70 °C, which is about 15 degrees higher than the T_m obtained for Myc1245 G4 and Pu27-G17A G4 (see SI, "Circular dichroism spectroscopy", Figure S1).

In our single-molecule manipulation experiments, a single-stranded c-MYC G4-forming sequence spanned between two dsDNA handles is tethered between a coverslip and a strepatavidin coated paramagnetic bead (Dynabeads M-280) (Figure 2A). The change in the average end-to-end distance of the construct (i.e., the extension) is measured at nanometer resolution based on the diffraction pattern of the bead image (see SI, "Materials and methods", for further details).[11,13]

Figure 2B shows typical force–extension curves obtained by a force-increase scan at loading rate r = 0.2 pN/s followed by a force-decrease scan at r = −0.2 pN/s (SI, "Force–extension curves", Figure S2). The force-increase curve (cyan) is below the force-decrease curve (gray) in the force range of 10–48 pN. We chose such a low loading rate to ensure that unfolding would occur at forces below 60 pN, to avoid interference from the DNA overstretching transitions of the dsDNA handles that typically occur at >60 pN.[14] The extension jump at ∼48 pN in the force-increase curve indicates an unfolding transition of the G4 (SI, "Specific control of G4 unfolding signal", Figure S3). After each force-scan cycle, the DNA molecule was held at a low force of ∼1 pN for 30 s to allow refolding. Successful refolding was indicated by the unfolding step in the subsequent force-increase scan.

The unfolding force distribution $p_{unfold}(f)$ could be obtained by recording the forces at which unfolding occurred. Figure 2C shows $p_{unfold}(f)$ of wt Pu27 for a total of 161 unfolding events obtained from more than 20 independent DNA molecules. It revealed two apparent force peaks centered at ∼22 and ∼50 pN, respectively, which is consistent with the existence of multiple G4 structures of Pu27 reported in previous gel electrophoresis analysis[7] and NMR measurements.[12a] The higher unfolding force specie is the major form, occupying ∼80% of the total population.

The unfolding force distribution was analyzed by Bell's model which describes the force-dependent unfolding rate as

$$k_u(f) = k_u^0 \exp(\Delta x_u f / k_B T) \quad (1)$$

where k_B is the Bolzman constant, T is absolute temperature, k_u^0 is the zero force unfolding rate, and Δx_u is the transition distance to the transition state. It predicts an unfolding force distribution with a single force peak $p_{unfold}^{Bell}(f)$ as

$$p_{unfold}^{Bell}(f) = \frac{k_u^0}{r} \exp\left\{\frac{\Delta x_u f}{k_B T} + \frac{k_B T k_u^0}{\Delta x_u r}\left[1 - \exp\left(\frac{\Delta x_u f}{k_B T}\right)\right]\right\} \quad (2)$$

where r is the loading rate.[15] The two parameters k_u^0 and Δx_u were treated as fitting parameters in our comparison.

The unfolding force of Pu27 shows two peaks. Best fitting to the measured $p_{unfold}(f)$ with combination of two unfolding force species $\alpha p_{major}^{Bell}(f) + (1-\alpha) p_{minor}^{Bell}(f)$, we determined Δx_{u1} = 0.8 ± 0.1 nm and $k_{u1}^0 = (1.4 \pm 1.0) \times 10^{-6}$ s^{-1} (average ± standard error) for the major specie, and Δx_{u2} = 0.8 ± 0.1 nm and $k_{u2}^0 = (1.2 \pm 0.3) \times 10^{-3}$ s^{-1} for the minor specie, as well as the fraction of the major form α, ∼78%.

The measured $p_{unfold}(f)$ for Myc2345 G4 shows a single-peaked unfolding force distribution (Figure 2D). Best-fitting to eq 2 determined best-fitting parameters as $k_u^0 = (2.6 \pm 0.6) \times 10^{-6}$ s^{-1} and Δx_u = 0.77 ± 0.02 nm. It has been known that this

DOI: 10.1021/ja511680u
J. Am. Chem. Soc. 2015, 137, 2424–2427

mutant can form four isoforms with small difference in loop regions.[12c] The single-peaked $p_{unfold}(f)$ indicates that either one isoform predominates the folding or these isoforms have similar mechanical stability. The $p_{unfold}(f)$ of Myc2345 G4 nearly overlaps with that of the major specie of Pu27 G4. However, our detailed unfolding step analysis revealed that the Myc2345 unfolding step size is slightly shorter (~2 nm) than that of the wt Pu27 (SI, Figure S4), implying that in addition to the core G tracts 2, 3, 4, and , the G tract 1 and the last 2 G nucleotides may also participate in the folded structures. $p_{unfold}(f)$ of Myc1245 and Pu27-G17A show widespread unfolding forces, suggesting that these mutants can form a variety of folded structures with similar probabilities. Due to the spread nature of their unfolding forces, we did not attempt to fit the data with Bell's model.

We next sought to determine the refolding probability $p_{fold}(t)$ as a function of time. To obtain $p_{fold}(t)$ at a constant force, we used a force-jump procedure, in which force was switched between a higher value of ~54 pN to mechanically unfold the G4 and a lower value of ~1 pN for G4 refolding (Figure 3A).

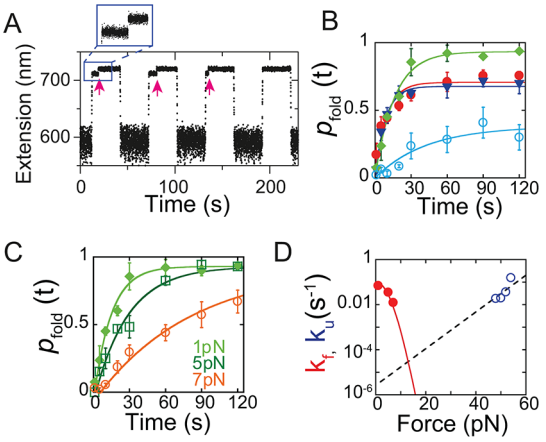

Figure 3. Unfolding and folding kinetics. (A) Force-jump experiments. Force jumping between 1 and 54 pN. G4 folding at 1 pN was detected from the unfolding step (red arrow) in the subsequent 54 pN holding. (B) The time evolutions of the folding probability of wt Pu27 (red), Myc2345 (green), Myc1245 (blue), and Pu27-G17A (cyan). Each data point was obtained from more than 80 times of force-jump cycles using three independent DNA tethers. (C) The time evolutions of the folding probability $p_{fold}(t)$ of Myc2345 at 1, 5, and 7 pN. (D) Force dependent folding rates k_f of Myc2345 estimated from fitting of $p_{fold}(t)$ and the unfolding rates k_u estimated from the lifetime analysis of G4 held at 48−54 pN. The dashed line is Bell's model predicted curve using parameters $k_u^0 \approx 2.6 \times 10^{-6}$ s^{-1} and $\Delta x_u \approx 0.77$ nm determined from the unfolding force distribution under constant loading rate. Error bars in (B) and (C) indicate standard errors.

In our instrument, it took <0.3 s for jumping from one force value to another. G4 unfolding at 54 pN was indicated by a 9 ± 2 nm stepwise extension increase (Figure 3A, red arrows and inset), and successful refolding occurred at 1 pN during the holding time t is indicated by an unfolding step at 54 pN after a subsequent force jumping. Repeating such force-jump cycles N times at a certain holding time t at 1 pN, we were able to obtain $p_{fold}(t) = M/N$, where M is the number of observed successful folding events.The measured folding probability showed strong dependence on KCl concentration supporting the formation of G4 structures (SI, "Effects of K^+ on Myc2345 G4 formation", Figure S5).

$p_{fold}(t)$ obtained for Pu27 and three mutants are shown in Figure 3B. The folding rate at 1 pN, $k_f(f = 1pN)$ of each construct was obtained by fitting to $p_{fold}(t)$ with exponential functions (Figure 3B). The fitted values for Pu27, Myc2345, and Myc1245 are similar, ranging 0.06−0.1 s^{-1}. Pu27-G17A has the slowest folding rate of 0.02 s^{-1}. It should be noted that this method can only detect mechanically stable structures. Less stable structures were likely unfolded during ~0.3 s force-jumping, as a result that their unfolding might not be observed at ~54 pN. For all constructs, $p_{fold}(t)$ reaches a steady state within 120 s, with saturation values of ~71%, ~93%, ~69%, and ~38% for Pu27, Myc2345, Myc1245, and Pu27-G17A, respectively. The near one saturation folding probability of Myc2345 indicates that Myc2345 mainly forms mechanically stable G4 that can be detected at high force with less than 7% potential weak species that were missed. The ~71% of the saturate folding probability of Pu27 indicates that ~29% Pu27 structures are mechanically weak, which could be intermediate states or less stable G4 forms. We also analyzed folding probability in constant loading rate (2 pN/s) measurements after 1 pN folding for 30 s. The results obtained for Myc2345 are similar in both assays; while about 19% weak species for Pu27 were missed in force-jump assay. Similar mechanism can explain the ~69% saturation folding probabilities for Myc1245 and ~38% for Pu27-G17A. An alternative explanation is that there is a ~29% equilibrium probability of reversible unfolding occurred at 1 pN force for Pu27. However, given its slow unfolding rate (Figure 2), we reason that this is an unlikely scenario. The significant decrease of the folding probability of Pu27-G17A to ~38%, indicating that "*G*" base located in the G tract 4 is crucial for c-*MYC* G4 folding into mechanically stable form.

Using a similar force-jump approach with varying lower forces for refolding and higher forces for unfolding, we were able to obtain the force-dependent folding and unfolding rates. We focused our measurements on the Myc2345 G4 since the G-tracts 2, 3, 4, and 5 have been suggested to be involved in the major form of the wt Pu27 G4. Fitting the data of $p_{fold}^{Myc2345}(t)$ measured at three different forces (Figure 3C) by exponential function, we obtained the corresponding folding rates $k_f(f)$ at 1, 5, and 7 pN as 0.069, 0.035, and 0.012 s^{-1}, respectively.

The force-dependent folding rates, which are governed by the Arrhenius law, were derived based on the force responses of folded G4 and unfolded ssDNA (SI, "Force-dependent folding rate") and plotted in Figure 3D (red line). Note that the nonlinear dependence of k_f on f in semilog scale is a generic outcome from the flexible polymer elasticity of ssDNA. The single free parameter $k_f^0 = 0.1$ s^{-1} was determined by matching the predicted $k_f(f)$ curve with the data measured at the three force values. We also note that Bell's model (eq 1) is not suitable for describing the force-dependent folding kinetics, because $\Delta x_f(f)$ can no longer be approximated as a constant due to distinct force−extension curves between the flexible ssDNA and the rigid nearly folded transition state.

The force dependent unfolding rates $k_u(f)$ can be obtained by applying the Bell's model (eq 1) using the parameters $k_u^0 \approx 2.6 \times 10^{-6}$ s^{-1} and $x_u \approx 0.77$ nm determined from fitting the unfolding force distribution in Figure 2D. The Bell's model is applicable because the transition state is a nearly folded rigid structure with similar size to the natively folded G4 which is indicated by the small unfolding transition distance. The validity of the predicted $k_u(f)$ was further tested by comparing it with directly measured unfolding rates (i.e., the reciprocal of

DOI: 10.1021/ja511680u
J. Am. Chem. Soc. 2015, 137, 2424−2427

average lifetime of G4 measured at four large constant forces (48−54 pN) obtained in force-jump experiments). As shown in Figure 3D, the predicted curve (dashed line) based on the kinetics parameters determined in Figure 2D directly matched the unfolding rate data obtained in constant force unfolding experiments (dots) without needs for any parameter adjusting.

The force-dependent free energy difference between unfolded and folded Myc2345 G4 was determined by $\Delta G(f) = -k_BT \ln(k_u(f)/k_f(f))$, from which the zero force value was calculated to be ∼10.5 k_BT (∼6.2 kcal/mol), similar to the value reported from previous biochemical bulk measurements (∼7.6 kcal/mol).[9] It should be noted that the attachment to a bead and dsDNA handles may alter the folding/unfolding kinetics of G4[16] thus causing potential difference between single-molecule and bulk measurements.

In summary, we have shown that the wt c-*MYC* promoter Pu27 sequence can form multiple G4's, and the major form has an extremely slow unfolding rate in the order of 10^{-6} s^{-1} at zero force, which is several orders of magnitude slower than that of telomeric G4 (in the order of 10^{-2}−10^{-3} s^{-1}) obtained by similar mechanical unfolding.[10] The slow unfolding rates may give the c-*MYC* G4 an advantage to perform its gene-silencing function through acting as a kinetic barrier to transcription.

The c-*MYC* G4 sequence belongs to a more broad class of G4 forming sequences marked by the motif G_3NG_3 found in many other human oncogene promoter regions which have also been shown to preferentially form parallel-stranded G4 structures, such as VEGF, HIF-1α, c-KIT, RET, and PDGF-A.[17] Thus, our measurements of c-*MYC* G4 may provide a generic understanding of the stability of a broad class of parallel-stranded G4 and insights into their transcriptional inhibition functions. Finally, the formation of promoter G4 is in competition with formation of double-stranded duplex, which may be further regulated by the level of DNA supercoiling[18] and protein binding. Further studies in the presence of complementary strand and superhelicity condition are still required to fully underdtand the G4 stability and regulation *in vivo*.

■ ASSOCIATED CONTENT

Supporting Information

Materials and methods, and Figures S1−S5. This material is available free of charge via the Internet at http://pubs.acs.org.

■ AUTHOR INFORMATION

Corresponding Author

*phyyj@nus.edu.sg

Notes

The authors declare no competing financial interest.

■ ACKNOWLEDGMENTS

The authors thank Daniela Rhodes, Ahn Tuân Phan, Hanbin Mao, and Danzhou Yang for stimulating discussions, and Chen Lu for proofreading the manuscript. The work is funded by Singapore Ministry of Education Academic Research Fund Tier 3 (MOE2012-T3-1-001) and the National Research Foundation through the Mechanobiology Institute Singapore.

■ REFERENCES

(1) Sen, D.; Gilbert, W. *Nature* **1988**, *334*, 364.

(2) (a) Qin, Y.; Hurley, L. H. *Biochimie* **2008**, *90*, 1149. (b) Lipps, H. J.; Rhodes, D. *Trends Cell Biol.* **2009**, *19*, 414. (c) Balasubramanian, S.; Hurley, L. H.; Neidle, S. *Nat. Rev. Drug Discov.* **2011**, *10*, 261.

(3) Simonsson, T.; Pecinka, P.; Kubista, M. *Nucleic Acids Res.* **1998**, *26*, 1167.

(4) Miller, D. M.; Thomas, S. D.; Islam, A.; Muench, D.; Sedoris, K. *Clin. Cancer Res.* **2012**, *18*, 5546.

(5) Slamon, D. J.; deKernion, J. B.; Verma, I. M.; Cline, M. J. *Science* **1984**, *224*, 256.

(6) Berberich, S. J.; Postel, E. H. *Oncogene* **1995**, *10*, 2343.

(7) Siddiqui-Jain, A.; Grand, C. L.; Bearss, D. J.; Hurley, L. H. *Proc. Natl. Acad. Sci. U.S.A.* **2002**, *99*, 11593.

(8) Lane, A. N.; Chaires, J. B.; Gray, R. D.; Trent, J. O. *Nucleic Acids Res.* **2008**, *36*, 5482.

(9) Olsen, C. M.; Gmeiner, W. H.; Marky, L. A. *J. Phys. Chem. B* **2006**, *110*, 6962.

(10) (a) Koirala, D.; Dhakal, S.; Ashbridge, B.; Sannohe, Y.; Rodriguez, R.; Sugiyama, H.; Balasubramanian, S.; Mao, H. *Nat. Chem.* **2011**, *3*, 782. (b) Long, X.; Parks, J. W.; Bagshaw, C. R.; Stone, M. D. *Nucleic Acids Res.* **2013**, *41*, 2746. (c) You, H.; Zeng, X.; Xu, Y.; Lim, C. J.; Efremov, A. K.; Phan, A. T.; Yan, J. *Nucleic Acids Res.* **2014**, *42*, 8789. (d) Yu, Z.; Koirala, D.; Cui, Y.; Easterling, L. F.; Zhao, Y.; Mao, H. *J. Am. Chem. Soc.* **2012**, *134*, 12338.

(11) Chen, H.; Fu, H.; Zhu, X.; Cong, P.; Nakamura, F.; Yan, J. *Biophys. J.* **2011**, *100*, 517.

(12) (a) Phan, A. T.; Modi, Y. S.; Patel, D. J. *J. Am. Chem. Soc.* **2004**, *126*, 8710. (b) Ambrus, A.; Chen, D.; Dai, J.; Jones, R. A.; Yang, D. *Biochemistry* **2005**, *44*, 2048. (c) Yang, D.; Hurley, L. H. *Nucleosides Nucleotides Nucleic Acids* **2006**, *25*, 951.

(13) Gosse, C.; Croquette, V. *Biophys. J.* **2002**, *82*, 3314.

(14) (a) Fu, H.; Chen, H.; Zhang, X.; Qu, Y.; Marko, J. F.; Yan, J. *Nucleic Acids Res.* **2011**, *39*, 3473. (b) Zhang, X.; Qu, Y.; Chen, H.; Rouzina, I.; Zhang, S.; Doyle, P. S.; Yan, J. *J. Am. Chem. Soc.* **2014**, *136*, 16073.

(15) Evans, E.; Ritchie, K. *Biophys. J.* **1997**, *72*, 1541.

(16) (a) Wang, Q.; Ma, L.; Hao, Y.-H.; Tan, Z. *Anal. Chem.* **2010**, *82*, 9469. (b) Bai, H.; Kath, J. E.; Zörgiebel, F. M.; Sun, M.; Ghosh, P.; Hatfull, G. F.; Grindley, N. D. F.; Marko, J. F. *Proc. Natl. Acad. Sci. U.S.A.* **2012**, *109*, 16546. (c) Arora, A.; Nair, D. R.; Maiti, S. *FEBS J.* **2009**, *276*, 3628.

(17) (a) Chen, Y.; Yang, D. *Curr. Protoc. Nucleic Acid Chem.* **2012**, 17. (b) Sun, D.; Guo, K.; Rusche, J. J.; Hurley, L. H. *Nucleic Acids Res.* **2005**, *33*, 6070. (c) De Armond, R.; Wood, S.; Sun, D.; Hurley, L. H.; Ebbinghaus, S. W. *Biochemistry* **2005**, *44*, 16341. (d) Rankin, S.; Reszka, A. P.; Huppert, J.; Zloh, M.; Parkinson, G. N.; Todd, A. K.; Ladame, S.; Balasubramanian, S.; Neidle, S. *J. Am. Chem. Soc.* **2005**, *127*, 10584. (e) Guo, K.; Pourpak, A.; Beetz-Rogers, K.; Gokhale, V.; Sun, D.; Hurley, L. H. *J. Am. Chem. Soc.* **2007**, *129*, 10220. (f) Qin, Y.; Rezler, E. M.; Gokhale, V.; Sun, D.; Hurley, L. H. *Nucleic Acids Res.* **2007**, *35*, 7698.

(18) (a) Sun, D.; Hurley, L. H. *J. Med. Chem.* **2009**, *52*, 2863. (b) Selvam, S.; Koirala, D.; Yu, Z.; Mao, H. *J. Am. Chem. Soc.* **2014**, *136*, 13967.

DOI: 10.1021/ja511680u
J. Am. Chem. Soc. 2015, 137, 2424−2427